Comments on Inorganic Chemistry
Publication details, including instructions for authors and subscription information:
http://www.informaworld.com/smpp/title~content=t713455155

Coordination and Activation of Dioxygen

Russell S. Drago[a]; Barry B. Corden[a]; Alan Zombeck[a]
[a] Schoole of Chemical Sciences, University of Illinois, Urbana, Illinois

To cite this Article Drago, Russell S. , Corden, Barry B. and Zombeck, Alan(1981) 'Coordination and Activation of Dioxygen', Comments on Inorganic Chemistry, 1: 1, 53 — 70
To link to this Article: DOI: 10.1080/02603598108078080
URL: http://dx.doi.org/10.1080/02603598108078080

Coordination and Activation of Dioxygen

Investigations of cobalt dioxygen adducts have lead to a simple, unified description of these complexes. Extension of this description to other metal dioxygen adducts gives insight into the function of biological and catalytic systems. Taking advantage of the high oxidizing power of O_2 in a controlled and selective manner is an important goal of chemists. Knowledge of the perturbation made on O_2 by coordination to metals is essential to understanding ways to activate it.

Introduction

Oxygen carriers have sparked the interest of chemists and biologists for decades. Though this area of research has been reviewed extensively,[1-7] our research[8] is focused on understanding how the geometric and electronic structure of these complexes affect their reactivity with dioxygen and how coordination affects the subsequent reactivity of dioxygen with organic substrates. By studying simple systems, better understanding of various means to overcome the kinetic inertness of oxygen can be developed and extended to designing and improving catalysts for industrial oxidations. Biological systems exhibit selectivity in oxidations with O_2 that is not readily attained in standard laboratory synthesis.

The research in our laboratory has proceeded along three different, though related, lines. One of these is the development of a molecular orbital scheme to represent the bonding in metal–dioxygen complexes which we call the 'spin-pairing model'. This model predicts that the partial charge on the dioxygen ligand varies substantially as the ligand field strength of groups coordinated to the metal is varied. Thus, one would predict a rich chemistry for the bound dioxygen.

We developed the spin-pairing model to explain the origin of the anisotropic cobalt hyperfine observed in the EPR experiment (*vide infra*). We felt that this hyperfine interaction could not be adequately explained by the

Comments Inorg. Chem.
1981, Vol. 1, pp. 53–70
0260–3594/81/0101–0053$06.50/0

prevalent formulation of these complexes as ionically bound superoxides. As a consequence of resolving this shortcoming, valuable insights about the factors influencing the metal–dioxygen bond strength, as well as the metal-catalyzed activation of O_2, have been realized.

The dioxygen-binding aspect of our investigations has involved the measurement of the thermodynamics of metal–axial base and metal–dioxygen bond formation. We have found that these systems fit the E and C equation, are understood in terms of the spin-pairing model, and have implications on the cooperativity of hemoglobin. At present, we are conducting mechanistic studies of dioxygen adducts of cobalt–Schiff-base complexes in catalytic systems; ultimately we hope to take advantage of the rich chemistry of bound dioxygen envisioned from the spin-pairing model for these systems.

The Structure of Co–O_2: A Free-Radical Picture

Cobalt and iron are the only metals reported to date that form all three geometries of metal–dioxygen complexes: the end-on bound mode (a),[1] the bridged species (b),[1] and the ring-bonded mode (c),[9] shown below.

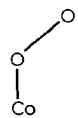

(a)

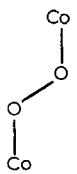

(b)

(c)

The reaction between low-spin cobalt(II) and dioxygen to form (a) can be viewed as a simple free-radical reaction in which the unpaired electron on the cobalt pairs with an unpaired electron on the dioxygen, leaving a single unpaired electron in the system.[10] This free radical cobalt–dioxygen adduct can then react in a second step with a second cobalt(II) to form the diamagnetic bridged species:

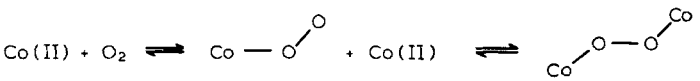

The formation of the ring-bonded mode with cobalt(I) can be viewed as involving the promotion of an electron from the d_{z^2} orbital of the d^8 species to the $d_{x^2-y^2}$ orbital. The two unpaired electrons in this excited configuration spin

pair with the two unpaired electrons on O_2 to produce the diamagnetic adduct shown below:

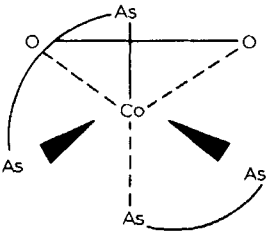

Our research is centered primarily on fundamental studies of end-on bound cobalt–dioxygen. We have recently demonstrated that both five- and six-coordinate type (a) complexes of cobalt(II) can be readily prepared.[11] It was previously supposed that four-coordinate cobalt complexes required an axial base before they could bind O_2, but these novel five-coordinate $Co–O_2$ complexes clearly demonstrate that this is not the case. This study[11] also demonstrated that electron transfer to form a formal cobalt(I) species is a requirement for forming type (c) adducts of dioxygen.

Spin-Pairing Model

The essence of the spin-pairing model involves classifying the metal–dioxygen interaction as a typical free-radical coupling reaction. In the case of low-spin cobalt(II), the unpaired electron of the metal (d^7) pairs up with an unpaired electron of dioxygen to form a bond. In other adducts, for example those of chromium(II) and iron(II), both electrons of dioxygen undergo this same type of spin-pairing, bonding interaction.

The application of the spin-pairing model to end-on bound dioxygen adducts of cobalt(II) is illustrated in Figure 1.

In a simplistic view, the adduct arises from the overlap of an oxygen π^* orbital with the Co $3d_{z^2}$ orbital to form a sigma bond, ψ_1. The other π^* orbital from the oxygen is orthogonal to d_{z^2} and remains and essentially O_2-based orbital, ψ_2. Neglecting the minor overlap of the oxygen orbital contribution to ψ_2 with other metal orbitals (d_{xz} and d_{yz}) as well as the mixing of 4s and other d orbitals into the metal–oxygen sigma bond, ψ_1, the basis set of ψ_1, ψ_2, and ψ_3 has the form:

$$\psi_1 = \alpha(d_{z^2}) + \beta(\pi_1^*)$$

$$\psi_2 = \pi_2^*(a2p_1 + b2p_2)$$

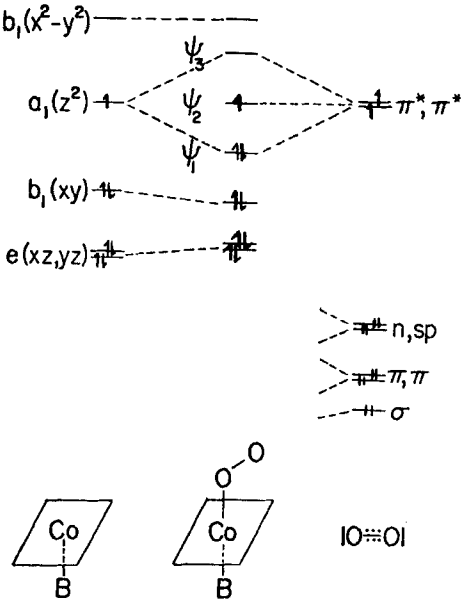

FIGURE 1 A molecular orbital diagram of the binding of dioxygen to five-coordinate Co(II). The unpaired electron in $Co(d_{z^2})$ spin pairs with an unpaired electron from O_2 to form ψ_1, leaving the remaining unpaired electron in ψ_2, an O_2-based orbital.

$$\psi_3 = \alpha(d_{z^2}) - \beta(\pi_1^*)$$

$$\beta = (1-\alpha^2)^{1/2}.$$

The significance of the coefficients α and β on the partial charge residing on the O_2 fragment is summarized in Table I. In sharp contrast to the earlier formulation of these complexes as metal-bound superoxide anions, the present model accomodates a range of charges from O_2^+ to O_2^-.

X-Ray Studies

The earlier formulation of the O_2 fragment as a bound superoxide was based on several experiments. One of these was the comparison of the O–O bond lengths from X-ray studies. The O–O bond length in molecular O_2 is 1.21 Å and for Co–O_2 complexes ranges from about 1.24 to 1.302 Å.[12a,b] This was compared to an erroneous value for KO_2 of 1.28 Å.[13a] Re-evaluation of the KO_2 data in 1962 has led to a value of 1.33–1.35 Å[13b] for the O–O bond length, which is supported by a value of 1.341 ± 0.010 Å from molecular photode-

TABLE I
The relation of the coefficients of ψ_1 to the nature of the O_2 adduct

α	β	Nature of O_2 adduct	Electron transfer[a]	ψ_1
0	1	$Co-O_2^-$	1.0	100% O_2
$\sqrt{2}/2$	$\sqrt{2}/2$	$Co-O_2$	0	50% Co, 50% O_2
1	0	$Co-O_2^+$	−1.0	100% Co

[a] Electron transfer $\simeq 2(1-\alpha^2)-1$. Note that the unpaired electron will reside in the O_2-based molecular orbital regardless of the extent of electron transfer.

tachment spectroscopy.[13c] Thus, from bond-length considerations, one would presume that there are varying amounts of electron transfer in the different $Co-O_2$ adducts. Unfortunately, such correlations can be misleading since the bond length could be affected by a variety of factors including lattice effects. The error limits on the O–O distance could also mask any trends in the data.

Infrared Studies

Infrared spectroscopy is an extremely useful method to distinguish between end-on adducts which have $\nu_{O\ O}$ stretching frequencies of about 1150 cm^{-1}, and the bridged and ring-bonded geometries which have a ν_{O-O} of about 800 cm^{-1}.[14] The insensitivity of ν_{O-O} to changes in the metal and ligands in the end-on bound systems and its similarity to ν_{O-O} for O_2^- (1097 cm^{-1})[4] have been used to support the description of dioxygen adducts as ionically bound superoxide. The fact that the O–O stretching frequency for the O_2 adducts of the metalloporphyrins Co(TpivPP)(1-MeIm)O_2 (1150 cm^{-1}), Fe(TpivPP)(1-MeIm)O_2 (1159 cm^{-1}),[15a,b] LiO_2 (1097 cm^{-1}),[17a] KO_2 (1146 cm^{-1}),[17b] RbO_2 (1141 cm^{-1}),[17b] and CsO_2 (1115 cm^{-1})[17a] are all similar and exhibit no discernible trend despite the large differences in the covalent character of the bonding in these systems, leads to the conclusion that the frequency is quite independent of the covalent character in the σ bond. Thus, we concluded[14] that infrared results should be limited to determining the structural geometry of metal–O_2 adducts.

Electron Paramagnetic Resonance Studies

Electron paramagnetic resonance (EPR) directly measures the unpaired electron density in paramagnetic systems and has provided the most information regarding the nature of the molecular orbital containing the unpaired electron in these adducts. The ^{17}O anisotropic hyperfine constant

indicates that the single unpaired electron in these systems resides in a molecular orbital composed primarily of oxygen p orbitals, ψ_2. The oxygens are inequivalent, possessing 40 and 60% spin densities on the middle and terminal oxygens, respectively.[18]

These are surprising results since the sum of the anisotropic ^{17}O and Co hyperfine coupling constants adds up to more than one unpaired electron in the system, even though only one is present. Thus, an indirect, rather than direct, mechanism must lead to negative spin density on the metal center and account for the cobalt hyperfine coupling in these systems. Evidently, the unpaired electron in ψ_2 can polarize the underlying Co 3d orbitals to produce the cobalt hyperfine coupling observed in the EPR. The pronounced variation in the cobalt hyperfine coupling constant in a series of O_2 adducts indicates extensive variation in the cobalt contribution to ψ_1 and thus in the nature of the bound O_2.[19]

The magnitude of the cobalt contribution to ψ_1 has been estimated by calculating a McConnell-type scaling factor to convert the anisotropic cobalt hyperfine coupling constant to the fraction of cobalt character in ψ_1. This can be related to the extent of electron transfer to the bound O_2. A list of adducts studied to date is given in Table II. The spin-pairing model predicts that as the donor strength of the ligands around the cobalt increases, the metal orbital containing the unpaired electron in the five-coordinate adduct is raised in energy relative to the π^* orbitals of O_2, and the complex becomes increasingly O_2^- in character. Accordingly, increasing electron transfer should be found on going from an N_2O_3 donor set to an N_5 donor set. When the very strong glyoximate donor ligand[20] is present, the electron transfer values are large. As indicated in Table II, these rough trends are subject to minor reversals due to complex, subtle electronic variations in different systems, such as varying amounts of 4s orbital admixture in ψ_1. In the low symmetry of many of these dioxygen adducts, other d orbitals can also be mixed into ψ_1. In both the cobalt porphyrin[21] and dimethylglyoxime complexes, axial base variation leads to lower values of electron transfer as the base strength increases. If this results from variation in the d orbital mixing into ψ_1, the actual electron transfer is even less than our semiquantitative estimate. These minor trends are not fully understood; however, it is clear that pronounced changes in the extent of electron transfer into the dioxygen moiety exist in the series of compounds in Table II.

Recent single crystal studies of $CoMbO_2$ (Mb = myoglobin)[22] and the O_2 adduct of vitamin B_{12}[23a-c] indicate that the largest component of the cobalt hyperfine tensor lies near the corrin ring or porphyrin plane. This observation would suggest either direct delocalization of the unpaired electron into d_{xz} or d_{yz} (π backbonding) or in terms of the indirect mechanism, a significant mixing of the d_{xz} or d_{yz} orbitals into ψ_1. The lowered symmetry of the O_2 adduct would

TABLE II
Electron transfer in some O_2 adducts of cobalt(II) complexes

Compound[a]	Electron transfer[b]	Donor set
Co(acacen)·H_2O·O_2	0.1	
Co(X-salDAPE)·O_2		
X = 5 – H	0.2	N_2O_3
X = 5 – OMe	0.3	
X = 5 – Br	0.3	
Co(acacen)·py·O_2[c]	0.4	
Co(salen)·py·O_2	0.5	N_3O_2
Co(SMDPT)·O_2	0.5	
$Co(DPGB)_2$·HMPA·O_2[d]	0.7	N_4O
$Co(DPGB)_2$·acetone·O_2[d]	0.8	
Co(PPIXDME)·py·O_2	0.5	
Co(*p*-OCH_3TPP)·py·O_2[c]	0.6	
Co(*p*-OCH_3TPP)(1-MeIm)O_2	0.5	N_5
Co(DMGH)·py·O_2[d]	0.7	
$Co(DPGB)_2$·CH_3CN·O_2[d]	0.8	

[a] Abbreviations: acacen, *N,N'*-ethylenebis(acetylacetoimine); salen, *N,N'*-ethylenebis(salicylidenimine); SMDPT, bis(salicylidene-γ-iminopropyl)methylamine; DMGH, dimethylgloxime; DPGB, BF_2-capped diphenylglyoxime; X-salDAPE, bis(salicylidene)diaminopropyl ether; *p*-OCH_3TPP, *p*-methoxyphenyl-*meso*-tetraphenylporphyrin; PPIXDME, protoporphyrin(IX) dimethyl ester; HMPA, hexamethylphosphoramide; py, pyridine.

[b] Electron transfer from Co(II) to O_2. The results are semiquantitative.[19]

[c] Molecular Orbital calculations on these systems agree with our electron tansfer values.[24b]

[d] The high electron transfer values for the oxime donors are expected since oximes generate about the same ligand field strengths as cyano compounds.[20]

[e] The electron transfer values tend to be *upper limits.*

permit this sort of mixing. The π-backbonding argument is inconsistent with two important observations. First, the magnitude of the anisotropic ^{17}O hyperfine coupling constant indicates that one unpaired electron resides on the dioxygen. Delocalization of the unpaired electron onto cobalt should have resulted in less $A_{^{17}O}$ than one unpaired electron on the dioxygen. The value of the anisotropic ^{17}O coupling constant observed is larger than expected for this interpretation. Second, the trend in the cobalt anisotropic hyperfine coupling constant with ligand field strengh is opposite to that predicted for a π-backbonding mechanism when the M–O–O angle is constant. If π-backbonding were extensive, the magnitude of the cobalt anisotropic hyperfine coupling constant would increase as the ligand field strength increases. A better cobalt–oxygen energy match (increased ligand field strength) would mix more of the cobalt d_{xz} (or d_{yz}) orbital into ψ_2 and increase the cobalt A_{aniso} value. This is not observed.[19]

TABLE III
Experimental enthalpies of base and dioxygen binding to Co(PPIXDME)

Base	$-\Delta H^0_{1:1}$ (kcal mol^{-1})	$-\Delta H_{O_2}$ (kcal mol^{-1})
N-Methylimidazole (NMeIm)	9.6	10.0 (0.2)[a]
Pyridine	8.9	8.0 (0.4)
Hexamethylphosphoramide (HMPA)	8.9	8.9 (0.2)
N,*N*-dimethylacetamide (DMA)	7.4	6.6 (0.7)
Tetrahydrothiophene (THTP)	6.0	7.6 (0.6)

[a] Numbers in parenthesis are error limits.
$-\Delta H^0_{1:1}$, enthalpy of formation of five-coordinate base adduct.
$-\Delta H_{O_2}$, enthalpy of formation of six-coordinate dioxygen adduct.

Molecular Orbital Calculations

This empirically derived spin-pairing model is supported by numerous molecular orbital calculations at various levels of approximation.[24a-g] One in particular, an INDO–UHF calculation[24b] on Co(acacen)·NH_3·O_2, agrees with EPR results that 0.38 and 0.61 unpaired electrons reside on the middle and terminal oxygens, respectively, with negative spin density in the Co $3d_{z^2}$ and 4s orbitals, and with very small spin density in d_{xz} and d_{yz}. This coincides with the view that ψ_2 is essentially oxygen-based with very little unpaired electron spin delocalized from ψ_2 to the metal π orbitals, and that the anisotropic cobalt hyperfine coupling arises from spin polarization. Finally the extent of electron transfer from Co to O_2 is calculated to be 0.3 e^-, compared to our upper limit of 0.4 e^- from the EPR analysis of Co(acacen).py.O_2.

Influence of Ligands on Metal Binding of O_2

The enthalpies of dioxygen binding, ΔH_{O_2}, (see Table III) parallel[25] the strength of axial base coordination ($\Delta H_{1:1}$) in a series of five-coordinate cobalt(II) protoporphyrin IX dimethyl ester [Co(por)] complexes. As the enthalpy of axial base interaction becomes more negative in a series of Co(por) base adducts, the metal orbitals are driven higher in energy relative to the oxygen π^* orbital. The higher the initial energy of the metal orbitals in the five-coordinate adduct, the more the electrons in them are stabilized upon forming the bond to O_2.

These thermodynamic data were incorporated into the *E* and *C* equation:[23]

$$-\Delta H = E_A E_B + C_A C_B,$$

so that enthalpies of dioxygen adduct formation can be predicted for Co(por)·B with any of the 51 bases whose E_B and C_B parameters have been reported. The following equation can be derived[23] for predicting the enthalpies of dioxygen binding to Co(por)·B:

$$-\Delta H_{O_2} = 7.3\ E_B + 1.2\ C_B + 1.5. \quad (1)$$

The -1.5 kcal mol^{-1} corresponds to the enthalpy change for the reaction:

$$\text{Co(por)} + O_2 \rightarrow \text{Co(por)}O_2. \quad (2)$$

Thus our understanding of the factors influencing O_2 binding to this porphyrin has progressed to the point where they can be quantitatively predicted from the base E_B and C_B properties. Since the relative importance of the covalent property of the base is slightly more important in forming a dioxygen adduct than in forming a Co(por), 1:1 base adduct ($E_A = 4.44$, $C_A = 0.58$), the higher enthalpy of O_2 binding to the tetrahydrothiophene adduct than to the dimethylacetamide adduct is understood (see Table III).

The E and C treatment would not work for bases in which there are steric effects involved in the cobalt–base interaction or those in which the ligand has π-acceptor properties. The predictability of the behaviour of the 1-methylimidazole systems with the E and C approach clearly indicates, that, contrary to previous literature reports,[26a,b] π-bonding effects do not account for the strong dioxygen binding properties of this axial base.

The axial base variation in the porphyrin series is expected to have a pronounced influence on the d_{z^2} orbital energies leading to a simple interpretation of the binding trends. The higher the energy of this orbital in the five-coordinate adduct, the more the electron in this orbital is stabilized by occupying the bonding molecular orbital ψ_1 in the adduct and the larger the measured enthalpy of O_2 binding. It would be improper to extrapolate these conclusions directly to the lower symmetry complexes which arise from equatorial base variation, for example, to compare porphyrins with Schiff-base complexes. Experiments are underway to determine the influence of these changes.

Other Metal Ion Complexes

The spin-pairing model can be used to predict the electronic ground state and the magnetism of end-on and triangular O_2 adducts of other transition metals. In the O_2 adducts of iron(II), chromium(II), and manganese(II), unpaired electrons in metal-based orbitals permit spin pairing with both π^* electrons of

O_2 (see Figure 2). Although molecular orbital calculations show extensive mixing of the d orbitals upon adduct formation, the spin-pairing model still provides a good working model. We begin with a description of the iron complex.

Low or intermediate spin, square planar, four-coordinate iron(II) complexes can coordinate an axial base leading to a high spin complex. The systems that pick up O_2 reversibly require base coordination. A low spin, diamagnetic O_2 adduct results as shown (see Figure 2c) when the d_{z^2} orbital in the O_2 adduct is driven up in energy via the strong interaction of O_2 with this orbital.[27a,b] A paramagnetic O_2 adduct of iron(II) is predicted if a ligand field were employed that led to a decreased $d_{x^2-y^2}$ and d_{z^2} separation in the adduct. A weak interaction with O_2 could also lower the d_{xz}–O_2 or d_{yz}–O_2 antibonding orbitals to such an extent that they become populated and a paramagnetic adduct results. A paramagnetic dioxygen adduct of iron(II), in which the unpaired spin is contained in essentially metal-based orbitals, is attainable in the context of the spin-pairing description. The guide lines offered for the synthesis of such a species constitute a valuable contribution of this model. The recent report[28a,b] of a thermally populated paramagnetic state of hemoglobin is readily accommodated by these considerations, but the absence of a contact-shifted NMR in this system is surprising.

Similar application of the spin-pairing model describes the reported O_2 adducts of Cr(II) (see Figure 2a). After the spin-pairing interaction of two metal electrons of the d^4 configuration with both of the O_2 π^* electrons, the CrO_2 adduct is predicted to contain two metal-based electrons as found experimentally. Lower symmetry ligand fields of appropriate strength could lead to a diamagnetic adduct.

The EPR and magnetic properties[30a] of the reported O_2 adducts of Mn(II) are also consistent with the predictions of the spin-pairing model (see Figure 2b). It is not known whether this adduct is a type (a) or type (c) complex. For both geometries, the adduct will have three metal-based, unpaired electrons.[30b] Again by proper ligand design, a low-spin O_2 adduct with one metal-based, unpaired electron could result. Thus the spin-pairing model we propose can account for the electronic structure of a wide variety of O_2 adducts.

Implications of These Results to Biological Systems

It is quite evident upon examination of the literature that thermodynamic quantities such as $-\Delta H_{O_2}$ for porphyrin adducts can differ profoundly from biological analogs.[31a] The factors that affect metal–dioxygen bond strengths in hemoglobin are difficult to intepret due to competition from a variety of

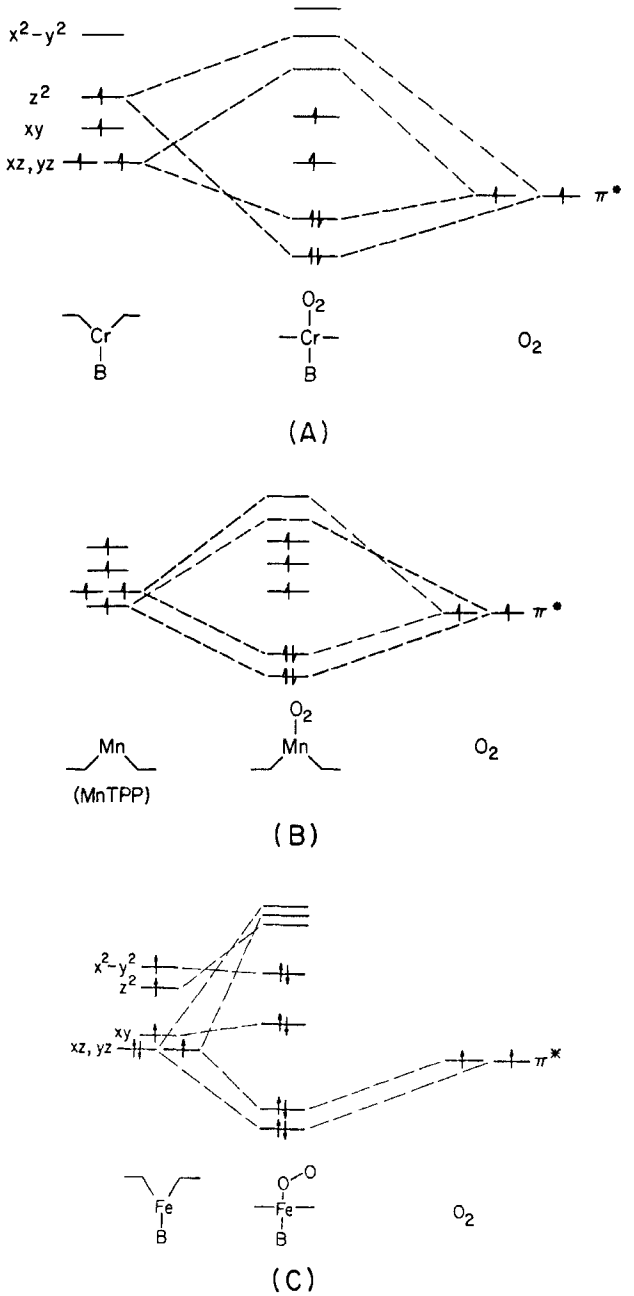

FIGURE 2 Molecular orbital diagram for O_2 adducts of Cr(II), Mn(II), and Fe(II) showing spin pairing upon adduct formation.

different ionization reactions that occur simultaneously. For example, the data for hemoglobin systems exhibit a pronounced pH dependence referred to as the Bohr effect. The variation in oxygen binding affinities for *meso*-, *deutero*- and *proto*- hemoglobins is considerably larger than that expected for these substituents on the prophyrin. Substitution of iron by cobalt in myoglobin results in a 2.3 kcal mol^{-1} *decrease* for the *meso*-protein, a 1.4 kcal mol^{-1} *increase* for the *deutero*-protein, and either a 3.0 or 1.6 kcal mol^{-1} *decrease* for the *proto*-protein compared to the iron system.[31b] Full understanding of the factors influencing the energetics of these biological systems is indeed a formidable problem.

Cooperativity in Hemoglobin

To a first approximation, the spin-pairing model predicts that dioxygen binding will become weaker as the strength of the axial base bound to a metal becomes weaker. The same trends observed in the Co(II)(PPIXDME) system should also apply to the iron(II) systems, because the higher the energy of the metal electrons in a five-coordinate adduct the greater the stabilization upon binding O_2. These considerations have important implications regarding the mechanism of cooperativity in the hemoglobin system. Hemoglobin has two different quaternary structures: the R state and T state. The O_2 affinity of the R state is essentially that of the isolated subunits, while that of the T state is significantly lower. The iron is displaced out of the plane toward the coordinated (proximal) histidine in the five-coordinate, deoxy T form. Movement of the proximal histidine toward the iron cannot be accomplished without a change in protein conformation.[32a,b] This restraint leads to a weakened iron–histidine interaction in the O_2 adduct. As shown by the enthalpies of oxygenation of cobalt(II)protoporphyrin(IX) dimethyl ester and as predicted by the spin-pairing model, a weakened proximal imidazole–iron interaction will lower the oxygen-binding affinity. The protein could cause a bond lengthening or a bent metal–nitrogen bond, preventing direct overlap of the histidine nitrogen with the iron d_{z^2} orbital (see Figure 3). The *E* and *C* values of $Co(por)O_2$ and Co(por) indicate that the former is nearly twice as good a Lewis acid as the latter. Shorter metal–base distances are expected toward the stronger acid. By analogy with the cobalt system, the metal–proximal-imidazole interaction is expected to decrease upon oxygenation of the iron. Inhibition of a bond length decrease, or bending of the metal–nitrogen bond by the protein, would weaken the metal–histidine bond strength and lower the dioxygen binding affinity. EXAFS experiments[32c] show very small changes in the iron–porphyrin distances upon oxygenation. Similar iron–porphyrin bond lengths (within 0.02 Å) were found in low-affinity deoxy HbA and high-

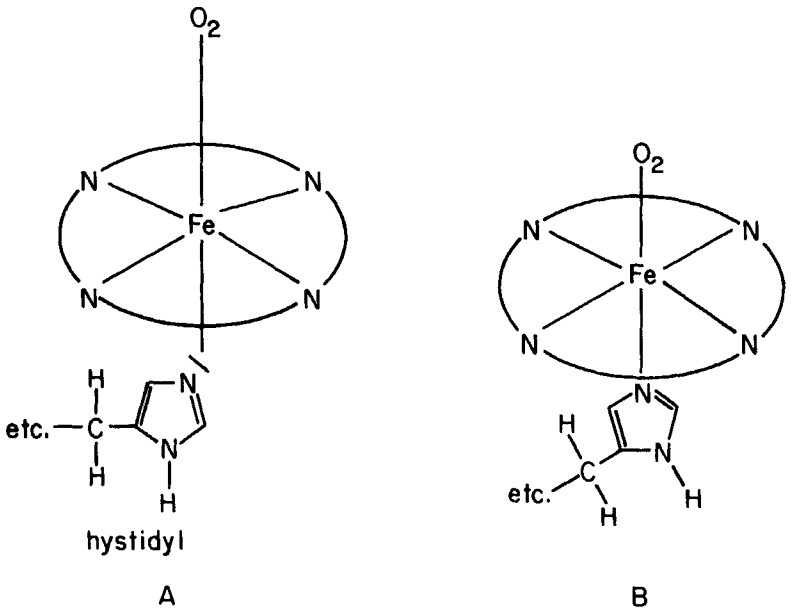

FIGURE 3 (a) Corresponds to the T state. A longer Fe–histidyl and Fe–O_2 bond denotes a weaker O_2 adduct. (b) Corresponds to the R state. A stronger, high-affinity, Fe–O_2 interaction occurs, reflected in a shorter Fe–O_2 bond.

affinity deoxy Hb Kempsey, indicating that weakened iron–histidine interaction is introduced in the T form upon oxygenation. These considerations suggest a potential energy storing model for cooperativity.

A weakened iron–proximal-histidine interaction results in weaker iron–nitrogen and metal–dioxygen bonds in the T form than would result in the absence of the restraint. As a result, coordination of dioxygen stores potential energy in the tetramer that could be released if the iron–nitrogen restraint were removed by a protein conformational change. The required energy for the protein change is not generated upon binding the first dioxygen. Multiples of this potential energy are stored on binding the second and third dioxygens. Note that potential energy is stored from a stronger metal–base interaction as well as a stronger dioxygen interaction for each bound oxygen. When the third dioxygen coordinates, more than enough potential energy is available in the system (from the increased iron–nitrogen and iron–O_2 bond strengths of the R form) to effect the endothermic T to R protein transformation. The fourth dioxygen is expected to be the most strongly bound (most exothermic) because in this step (see Figure 4) the O_2 coordinates to an iron in the R form.

In this view, all of the structural changes in the iron relative to the porphyrin are similar in Hb to those observed in systems not exhibiting cooperativity;

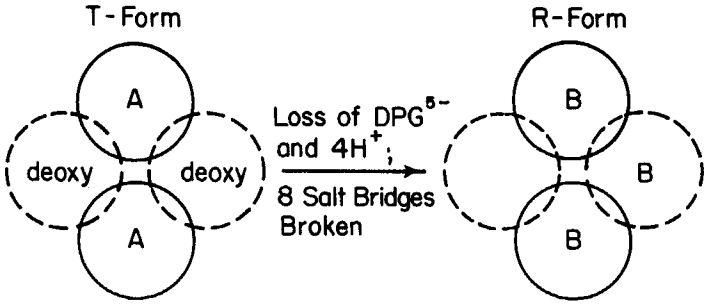

FIGURE 4 Schematic diagram of hemoglobin conformation change. A and B correspond to the heme units depicted in Figures 3a and 3b.

hence, the proximal imidazole interaction and the potential energy storing feature is the key to cooperativity. It is difficult to bookkeep the 3.5 kcal mol^{-1} difference in the O_2 binding affinity of high- and low-affinity forms. The endothermic T to R protein transformation, plus the 3.5 kcal mol^{-1}, is distributed over the three metal–oxygen, three iron–proximal-imidazole and twelve iron–porphyrin nitrogen interactions of the O_2 adducts. In view of the preceding discussion, we see the complexity of any mechanistic questions one may ask about cooperativity. The potential energy storing model provides a degree of understanding sufficient for many purposes.

Investigation of the Reactivity of Metal-Bound O_2

Clearly one of the most important tasks confronting researchers in this area involves probing the chemistry of metal-bound O_2 with the eventual goal of catalyzing selective oxidations with O_2. The experiments to date indicate that dioxygen gains electron density upon coordination to cobalt(II) and should be susceptible to attack by electrophiles.

We have recently performed an experiment in our laboratory[33] in which small amounts of 2,2,2-trifluoroethanol (TFE) is added to the dioxygen adduct of the five-coordinate CoSMDPT complex. Infrared studies of the O–H stretching vibration indicate that the TFE hydrogen bonds with coordinated dioxygen. An enthalpy–frequency shift relation provides an estimate of a 6.6 kcal mol^{-1} hydrogen-bonding interaction with O_2. Work is currently underway to determine whether the extent of electron transfer and ν_{OH} can be correlated to the catalytic activity of cobalt–dioxygen adducts.

The stabilization of CoSMDPT(O_2) by the hydrogen-bonding interaction with TFE may indicate that the enhanced stabilization of the O_2 adduct in CoMb and Co(TpivPP)(NMeIm) compared to Co(PPIXDME)(NMeIm) is

due to a hydrogen-bonding stabilization of the O_2 fragment by the protein or pickets that are not present in the flat prophyrin.[33]

Summary of Co–O_2 Oxidation of Hindered Phenols

Hindered phenols are oxidized to the corresponding benzoquinones by cobalt–dioxygen carriers.[34] This reaction is significant because it represents one of few examples where a metal–dioxygen adduct is involved in the mechanism. In many catalytic oxidations, a transition metal serves to catalytically decompose an alkyl hydroperoxide or act as an oxidizing agent. We have made significant observations leading to an increased understanding of oxidations by metal-coordinated O_2. First, a kinetic investigation[35] provided reaction orders, first order in [Co], [O_2], and [phenol]. Furthermore, cobalt complexes which do not reversibly bind O_2 [such as $Co(acac)_2$], do not catalyze the reaction. It was also shown that hydrogen-bonding acids stronger than phenol stopped the reaction even when they were added after the reaction was in progress. These results provide strong support for a reaction mechanism in which the first step is a hydrogen-atom abstraction by a coordinated O_2:

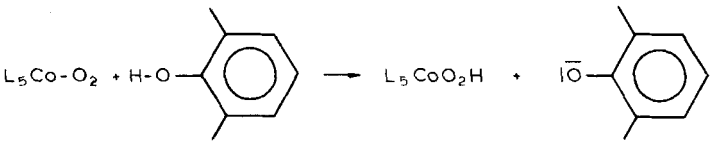

There are several subsequent pathways for the conversion of the phenoxy radical to the quinone. However, an EPR study has suggested that the reaction between a phenoxy radical and Co–O_2 may be an important route.

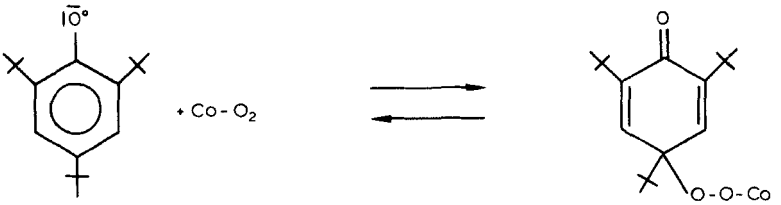

We can only speculate that, in the course of the 2,6-disubstituted phenol oxidation, the fate of the cobalt–peroxo compound is similar to that of an alkyl hydroxyperoxide.

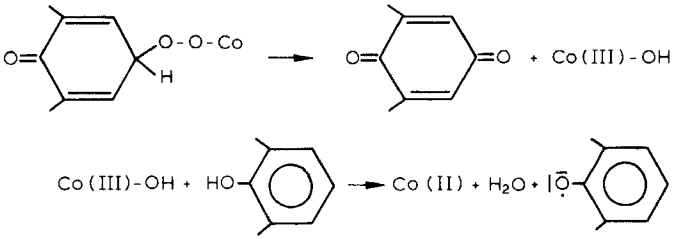

This mechanism is supported by oxidations with the 'heterogenized' polymer-attached CoSalMeDPT[36] oxidation catalyst. Both benzoquinone (BQ) and diphenoquinone (DPQ),

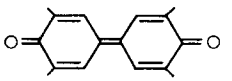

are obtained as products. When the cobalt concentration in the polymer catalyst is decreased, the BQ/DPQ ratio is decreased. This suggests that if the phenoxy radical does not encounter a $Co–O_2$ adduct, it dimerizes to form

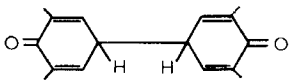

which is oxidized to DPQ. High selectivity toward BQ can be obtained at high cobalt(II) concentrations in the polymer.

Concluding Remarks

Taking advantage of the high oxidizing power of dioxygen in a controlled and selective manner is an important goal of chemists. When the bonding of metal–dioxygen complexes is viewed from the framework of the spin-pairing model, some elements of the knowledge essential to the understanding of dioxygen activation is provided.

Acknowledgment

We wish to thank our coworkers whose names appear in the references. This work is supported by the National Science Foundation.

RUSSELL S. DRAGO, BARRY B. CORDEN, ALAN ZOMBECK
Schoole of Chemical Sciences,
University of Illinois,
Urbana, Illinois 61801

References and Notes

1. J. S. Valentine, Chem. Rev. **73**, 235 (1973); and references therein.
2. G. Henrici-Olive and S. Olive, Angew Chemie Int. Ed. (Eng.) **13**, 29 (1974).
3. F. Basolo, B. Hoffman and J. Ibers, Acc. Chem. Res. **8**, 384 (1975).
4. L. Vaska, Acc. Chem. Res. **9**, 175 (1976).
5. G. McLendon and S. E. Martell, Coord. Chem. Rev. **19**, 1 (1976).
6. J. P. Collman, Acc. Chem. Res. **10**, 265 (1977).
7. R. D. Jones, D. S. Summerville and F. Basolo, Chem. Rev. **79**, 139 (1979).
8. R. S. Drago and B. B. Corden, Acc. Chem. Res. **13**, 353 (1980).
9. N. W. Terry, E. L. Amma and L. Vaska, J. Am. Chem. Soc. **92**, 653 (1972).
10. R. S. Drago, Coord. Chem. Rev. **32**, 97 (1980).
11. R. S. Drago, J. R. Stahlbush, D. J. Kitko and J. Breese, J. Am. Chem. Soc. **102**, 1884 (1980).
12. (a) L. D. Brown and K. N. Raymond, Inorg. Chem., **14**, 2595 (1975), for $[N(C_2H_5)_4]_3[Co(CN)_5CO_2]\cdot 5H_2O$; (b) A. Avdeef and W. P. Schaefer, J. Am. Chem. Soc. **98**, 5153 (1976), for Co(3-F-Saltmen)(1Me-Imid)$(O_2)\cdot 2(CH_3)_2CO$.
13. (a) S. C. Abrahams and J. Kalnajs, Acta Cryst. Camb. **8**, 503 (1955). (b) F. Halverson, Phys. Chem. Solids **23**, 207 (1962). (c) R. J. Celotta, R. H. Bennett, J. L. Hall, M. W. Siegel and J. Lerine, Phys. Rev. A **6**, 631 (1972).
14. R. S. Drago, Inorg. Chem. **18**, 1408 (1979).
15. (a) R. J. Blint and M. D. Newton, J. Chem. Phys. **59**, 6220 (1973). (b) M. E. Jacox and D. E. Milligan, J. Mol. Spec. **42**, 495 (1977).
16. J. P. Collman, J. I. Brauman, T. R. Halbert and K. S. Suslick, Proc. Natl. Acad. Sci. USA **69**, 2783 (1972).
17. (a) L. Andrews, 'IR and Ramon Spectroscopic Studies of Alkali–Metal–Atom Matrix Reaction Products', in *Cryochemistry*, ed. by M. Moskovits and G. A. Ozin, (John Wiley and Sons, Inc, New York, 1976). (b) F. J. Blunt, P. J. Hendra and J. R. Mackenzie, J. Chem. Soc. Chem. Comm. 278 (1969).
18. D. Getz, E. Melamud, B. L. Silver and Z. Dori, J. Am. Chem. Soc. **98**, 5144 (1976).
19. B. S. Tovrog, D. J. Kitko and R. S. Drago, J. Am. Chem. Soc. **98**, 5144 (1976).
20. E. I. Baucom and R. S. Drago, J. Am. Chem. Soc. **93**, 6469 (1971).
21. R. S. Drago, T. Beugelsdijk, J. A. Breese and P. Cannady, J. Am. Chem. Soc. **100**, 5374 (1978).
22. J. C. W. Chien and C. L. Dickinson, Proc. Natl. Acad. Sci. USA **69**, 2783 (1972).
23. (a) A. Schweiger, E. Jorin and H. H. Gunthard, Chem. Phys. Lett. **61**, 223 (1979). (b) E. Jorin, A. Schweiger and H. H. Gunthard, Chem. Phys. Lett. **61**, 228 (1979). (c) C. L. Dickinson and J. C. W. Chien, Proc. Natl. Acad. Sci. USA **77**, 1235 (1980).
24. (a) W. A. Goddard, III and B. D. Olafson, Proc. Natl. Acad. Sci. USA **72**, 2335 (1975). (b) P. Fantucci and V. Valenti, J. Am. Chem. Soc. **98**, 3832 (1976). (c) B. H. Huynh, D. A. Case and M. Karplus, J. Am. Chem. Soc. **99**, 6103 (1977). (d) R. V. Kirchner and A. H. Loew, J. Am. Chem. Soc. **99**, 4639 (1977). (d) A. Dedieu, M. M. Rohmer, M. Bernard and A. Veillard, J. Am. Chem. Soc. **98**, 3717 (1976). (f) A. Dedieu, M. M. Rohmer and A. Veillard, J. Am. Chem. Soc. **98**, 5789 (1976). (g) D. A. Case, B. H. Huynh and M. Karplus, J. Am. Chem. Soc. **101**, 4433 (1979).
25. The reported electron transfer values are semiquantitative. They are upper limits of the extent of electron transfer. The reader is urged to read the original paper[21] for a full explaination of how these values were obtained.
26. (a) F. A. Walker, J. Am. Chem. Soc. **95**, 1150 (1973). (b) D. V. Stynes, H. C. Stynes, J. A. Ibers and B. R. James, J. Amer. Chem. Soc. **96**, 1358 (1974); and references therein.
27. (a) L. Pauling and C. D. Coryell, Proc. Natl. Acad. Sci. USA **22**, 210 (1936). (b) J. P. Collman, J. I. Brauman, E. Rose and K. S. Suslick, Proc. Natl. Acad. Sci. USA **75**, 1052 (1978).
28. (a) M. Cerdonio, A. Congiu-Castellano, F. Mogno, B. Pispisa, G. L. Romani and S. Vitale, Proc. Natl. Acad. Sci. USA **74**, 398 (1977). (b) M. Cerdonio, A. Congiu-Castellano, L. Calabiese, S. Morant, B. Pispisa and S. Vitale, Proc. Natl. Acad. Sci. USA **75**, 4916 (1978).

29. S. K. Cheung, C. J. Crimes, J. Wong and C. A. Reed, J. Am. Chem. Soc. **98**, 5028 (1976).
30. (a) B. M. Hoffman, C. J. Weschler and F. Basolo, J. Am. Chem. Soc. **98**, 5473 (1976). (b) A. Dedieu and M. M. Rohmer, J. Am. Chem. Soc. **99**, 8050 (1977).

The authors in reference 30a concluded that $Mn–O_2$ is a type (c) adduct. Results of *ab initio* calculations[35b] indicate that a type (a) adduct should be significantly more stable than the type (c) conformation. These authors[35b] predict a $(O_2\pi)^2(O_2\pi)^1(d_{xy})^2(d_{yz})^1(d_{xz})^1$ ground state that is inconsistent with the ^{17}O EPR results.[35a] A better basis set and CI is not expected to enhance the stability of the type (c) over the type (a) adduct,[35b] but it could lead to a ground-state configuration with three metal-based unpaired electrons. An end-bonded dioxygen is consistent with the EPR results. We have chosen the energy level scheme in Figure 2b based on the above considerations.

31. (a) For example, $-\Delta H_{O_2}$ (kcal mol^{-1}) for OxyHb (Hb = hemoglobin) is 9.7 at pH = 6.8, 13.6 at pH = 9.5, and 15.6 for Fe(TpivPP)(1-MeIm) at pH = 7.0. [TpivPP = *meso*-tetra(α,α,α,α-*o*-pivalamidophenyl)porphyrin]. See F. J. W. Roughton, J. Biol. Chem. **29**, 2604 (1935); *ibid*, **30**, 2117 (1936); J. P. Collman, J. I. Brauman and K. S. Suslick, J. Am. Chem. Soc. **97**, 7185 (1975). (b) $-\Delta H_{O_2}$ (kcal mol^{-1}) for sperm whale Mb (Mb = myoglobin) at pH = 7.0 is 12.6 for the *meso*-, 8.9 for the *deutero*-, and 14.9 for the *proto*-porphyrin form. See A. Rossi Fannelli and E. Antonini, Arch. Biochem. Biophys. **73**, 243 (1957). By contrast, $-\Delta H_{O_2}$ (kcal mol^{-1}) for cobalt–Mb at pH = 7.0 is 10.3 for the *meso*-, 10.3 for the *deutero*-, 11.9 or 13.3 for the *proto*-porphyrin form. See T. Yonetani, H. Yamamoto and G. V. Woodrow, III, J. Biol. Chem. **249**, 682 (1974); C. A. Spillburg, B. M. Hoffman and D. H. Petering, J. Biol. Chem. **247**, 4219 (1972).
32. (a) M. F. Perutz, Br. Med. Bull. **32**, 195 (1976). (b) M. F. Perutz, Ann. Rev. Biochem. **48**, 327 (1979), and references therein. (c) P. Eisenberger, R. G. Shulman, B. M. Kincaid, G. S. Brown and S. Ogawa, Nature **274**, 30 (1978); and references therein.
33. R. S. Drago, P. Cannady and K. Leslie, J. Am. Chem. Soc. **102**, 6014 (1980).
34. H. M. Van Dort and H. J. Guerson, Rec. Trav. Chem. **86**, 520 (1967).
35. R. S. Drago, A. Zombeck, J. H. Gaul and B. Corden, submitted.
36. R. S. Drago, J. H. Gaul, A. Zombeck and D. Straub, J. Am. Chem. Soc. **102**, 1033 (1980).